Adaptive Modeling and Long-Range Prediction of Mobile Fading Channels

Abdorreza Heidari, *Student Member, IEEE*, Amir K. Khandani, *Member, IEEE*, and Derek McAvoy

Abstract

A key element for many fading-compensation techniques is a (long-range) prediction tool for the fading channel. A linear approach, usually used to model the time evolution of the fading process, does not perform well for long-range prediction applications. In this article, we propose an adaptive fading channel prediction algorithm using a sum-sinusoidal-based state-space approach. This algorithm utilizes an improved adaptive Kalman estimator, comprising an acquisition mode and a tracking algorithm. Furthermore, for the sake of a lower computational complexity, we propose an enhanced linear predictor for channel fading, including a multi-step linear predictor and the respective tracking algorithm. Comparing the two methods in our simulations show that the proposed Kalman-based algorithm significantly outperforms the linear method, for both stationary and non-stationary fading processes, and especially for long-range predictions. The performance and the self-recovering structure, as well as the reasonable computational complexity, makes the algorithm appealing for practical applications[1].

Index Terms

Wireless/Mobile Fading Channel, Channel Modeling, Channel Prediction, Sum-Sinusoidal model, State-Space Model, Kalman Estimation, Adaptive Filtering, Channel Tracking

Abdorreza Heidari and Amir K. Khandani are with the Coding and Signal Transmission Laboratory, ECE Department, University of Waterloo, Waterloo, Ontario, Canada. E-mails: {reza,khandani}@cst.uwaterloo.ca . Derek McAvoy is with Wireless Technology Strategy, Bell Canada, Mississauga, Ontario, Canada. Email: derek.mcavoy@bell.ca .

This paper in part [1] has been presented at the 23rd Biennial Symposium on Communication, May 2006. Moreover, the material presented in this paper is partly filed as a patent application [2].

[1]This work is financially supported by Bell Canada, Communications and Information Technology Ontario (CITO), and Natural Sciences and Engineering Research Council of Canada (NSERC).

I. INTRODUCTION

We address the problem of modeling and prediction of channel fading in this article. Channel fading prediction can be used to improve the performance of a wide range of telecommunication systems which employ channel state information (CSI). Having estimates of future samples of the fading coefficients enhances the performance of many tasks at the receiver and/or at the transmitter, including adaptive coding and modulation, channel equalization, the decoding process of data symbols, and antenna beamforming. In particular, the performance of adaptive coding and modulation techniques strongly depends on the performance of the fading prediction algorithm [3], and usually a long-range prediction algorithm is required [4]. Another application of the fading prediction is to compensate for the effect of feedback delay in closed-loop communication systems [5], [6]. This delay includes the effect of channel estimation, feedback calculation, feedback transmission, CSI reconstruction and application, and other processing delays. An extensive literature survey on the subject of fading modeling and prediction can be found in [4].

Consider a single-path flat fading channel from a transmit antenna to a receive antenna. The channel fading coefficient h_n is zero mean (subscript n is the time index), with the variance $\sigma_h^2 = 1$. Fig. 1 shows the block diagram for prediction of a fading channel. The channel coefficients are estimated from the received signal series $\{y_n\}$, where the nature of y_n could be different depending on the application. Usually y_n is a pilot signal which is appropriately designed for channel estimation, as in 3G systems. In some applications, y_n is the modulated user data which is used by a blind channel estimation algorithm. The subject of channel fading estimation is well-established in the literature and is not addressed here. We assume that the channel estimate $\overline{h}_n$ is shown as $\overline{h}_n = h_n + v_n$, where v_n is the estimation error modeled as a zero mean Gaussian noise with the variance σ_v^2. As an indicator for the estimation quality, the observation SNR is defined as $\mathrm{SNR}_z = \sigma_h^2/\sigma_v^2 = 1/\sigma_v^2$.

In this article, a single-path SISO fading channel is considered, and a novel Kalman-based adaptive predictor, as well as an enhanced adaptive linear predictor are proposed which are described later. If the path delay variations are not negligible in comparison with the symbol period, the same algorithms

could be applied to each resolved multi-path component, and also to every single channel in the case of a MIMO channel. However, it has been shown that MIMO channels can offer longer prediction lengths than traditional SISO channels [7]. An extension of the proposed Kalman-based method to the multi-path and multi-antenna case is presented in Appendix C. For the linear approach, there are conventional extensions available in the literature, for example see [8], [9].

For prediction of a future sample of the channel using the past measurements, a model is needed to represent the dynamics of the channel. Having the series of the channel measurements $\{\overline{h}_n\}$, the parameters of the model are estimated or updated, and the future fading sample is predicted as shown in Fig. 1. The model selection and extraction of the parameters, as well as the prediction algorithm, are explained in the sequel.

Many processes are represented with a linear model, i.e. an auto-regressive moving-average (ARMA) model. In this context, an approximate low-order AR model is often used as it can capture most of the fading dynamics. For example, see the MMSE linear predictor proposed in [10], and the channel tracking algorithms utilizing Kalman filter in [11] and [12]. Linear models are known to be optimal for Gaussian signals. Also linear models are easy to use and have a low complexity, however, they fail to show the true time behavior of a channel fading process. The Gaussian assumption for the fading signal is only valid for a rich-scattering area, i.e., when the number of dominant scatterers are significant. However, in many mobile environments, there are a few main scatterers which construct the fading signal [13]. Also the time-varying nature of the fading signal is in contrast with the Gaussian assumption in any case. Overall, the linear models do not perform well for long-range predictions as shown in the literature (for example, see [14]). The block-adaptive linear predictors are widely used, however for a fast time-varying channel (or for a long block length), the model parameters become outdated towards the block end. This problem can be ratified to some extent by updating the linear coefficients more frequently using adaptive methods [4]. Other than the linear approach, some other prediction approaches have been used for fading channels. For example, in [15], a linear-trend method is used in the context of multiuser detection. Article [14] uses a (nonlinear) quadratic approach and shows that while it has good modeling properties, it is very sensitive

to the model changes. Nonlinear methods have usually high complexities and they are hard to analyze. Furthermore, they are usually difficult to be adaptively applied. In this article, we utilize a nonlinear model as explained in the following. By applying an equivalent state-space model, we avoid the problems of nonlinear processing.

When the receiver, the transmitter, and/or the scatterers are moving, each scattered component undergoes a doppler frequency shift given approximately by [16]

$$f(k) = f_d \cos(\theta(k)) \tag{1}$$

where $\theta(k)$ is the incident radiowave angle of the k'th component with respect to the motion of the mobile and f_d is the maximum doppler frequency defined as $f_d = \frac{V}{C} f_c$, where f_c is the carrier frequency, V is the mobile speed and C is the speed of light. Assuming $N_{\rm sc}$ scatterers, the complex envelop of the flat fading signal at the receiver is

$$h(t) = \sum_{k=1}^{N_{\rm sc}} \rho(k)\, e^{j(\omega(k)\, t + \phi(k))} + \zeta(t) \tag{2}$$

where for the k'th scatterer, $\rho(k)$ is the (real) amplitude, $\phi(k)$ is the initial phase, $\omega(k) = 2\pi f(k)$, and $\zeta(t)$ is the model error. The phase $\phi(k)$ can be absorbed in the amplitude as $\alpha(k) = \rho(k)\, e^{j\phi(k)}$. According to (2), a fading channel can be modeled as sum of a number of sinusoids. This so-called sum-sinusoidal model relies on the physical scattering mechanism [17]. Previously, this model has been used for prediction of the channel fading [18], [19], [20], [21]. In this article, we use the sum-sinusoidal model in a Kalman filtering framework. This model is *adaptively* updated to follow the changes in the scattering environment. Unlike most of the works in the literature, we propose a complete adaptive modeling and prediction algorithm for time-varying fading channels. Also we present an enhanced adaptive linear algorithm, then compare their performance. It is shown here that how these two approaches behave and compare in a real situation with practical assumptions.

Assuming a two-dimensional isotropic scattering and an omni-directional receiving antenna, it is known that the autocorrelation function of the fading process can be written as [17]

$$R_h(t, t-\tau) = \frac{E[h(t)h^*(t-\tau)]}{\sigma_h^2} = J_0(2\pi f_d \tau), \tag{3}$$

where f_d is the maximum doppler frequency, $J_0(\cdot)$ is the first-kind Bessel function of the zero order, and τ is the time difference. A Rayleigh fading process with the above correlation property is called the Jakes fading [17], [22]. We examine the performance of the algorithms with the Jakes fading, and also with a non-stationary fading which is generated by a ray-tracing approach.

Here is a summary of the contributions of this article. In Section II, we propose a new linear prediction method. Conventionally a 1-step linear predictor is used. Here a D-step predictor (D$\geq$1) is presented, and the relation to the 1-step predictor is derived. This approach reduces the computational complexity of the conventional linear method. Furthermore, a tracking algorithm for coefficients of the D-step predictor is proposed. In Section III, we consider a state-space model based on the sum-sinusoidal fading model. Using the state-space model, an adaptive Kalman algorithm is proposed. The algorithm is presented for both acquisition and tracking phases. Additionally, a tracking algorithm for the doppler frequencies is proposed. Also we introduce an enhancement to the prediction part of the adaptive Kalman filter. In Section IV, the simulation results are presented and the algorithms are compared.

II. Linear Approach

To model a fading process, a linear model is widely used. An AR (Auto Regressive) model of order $N_{\rm AR}$ is recursively defined as follows

$$h_{n+1} \;=\; \sum_{i=1}^{N_{\rm AR}} a(i)\, h_{n-i+1} + \xi_{n+1} \tag{4}$$

where $\mathbf{a} = [a(1),\, a(2),\, \cdots,\, a(N_{\rm AR})]^T$ is the AR coefficients vector, and ξ_{n+1} is the model error which has a zero mean.

The time evolution of an AR model can also be shown as a state-space model [11], [9] as follows

$$\begin{cases} \mathbf{h}_n = \mathbf{B}\, \mathbf{h}_{n-1} + \mathfrak{q}_n \\ \\ z_n = \mathfrak{m}\, \mathbf{h}_n + u_n \end{cases} \tag{5}$$

where

$$\mathbf{h}_n = [h_n,\, h_{n-1},\, \cdots,\, h_{n-N_{\rm AR}+1}]^T \tag{6}$$

is the fading regressor at time n, $\mathbf{B}$ is the transition matrix defined as

$$\mathbf{B} = \begin{pmatrix} & \mathbf{a}^T & \\ \mathbf{I}_{N_{\rm AR}-1\times N_{\rm AR}-1} & & \mathbf{0}_{\mathbf{N_{AR}-1\times 1}} \end{pmatrix}, \tag{7}$$

and $\mathfrak{q}_n$ is the noise vector defined as $\mathfrak{q}_n = [\xi_n,\, \xi_{n-1},\, \cdots,\, \xi_{n-N_{\rm AR}+1}]^T$ representing the model error. $\mathfrak{m}$ is known as the measurement matrix which is defined as

$$\mathfrak{m} = [1,\, 0,\, \cdots,\, 0]_{1\times N_{\rm AR}}, \tag{8}$$

u_n is the observation noise, and z_n is the system output (which is substituted by the observed values for implementation).

It is easy to show that

$$\hat{\mathbf{h}}_{n+1|n} = \mathbf{B}\,\mathbf{h}_n, \tag{9}$$

where $\hat{\mathbf{h}}_{n+1|n}$ is the prediction of $\mathbf{h}_{n+1}$ given the observations up to the time n, i.e.,

$$\hat{\mathbf{h}}_{n+1|n} = E\left[\mathbf{h}_{n+1}|z_n,\, z_{n-1}\,\cdots\right]. \tag{10}$$

A. The Linear Prediction Algorithm (LP)

Assuming an AR model of the order $N_{\rm AR}$, a 1-step linear predictor is shown as follows

$$\hat{h}_{n+1|n} \;=\; \sum_{i=1}^{N_{\rm AR}} a(i)\,\overline{h}_{n-i+1}. \tag{11}$$

Minimizing the mean square error (MSE), $E\left[\left|h_{n+1} - \hat{h}_{n+1|n}\right|^2\right]$, provides the prediction coefficients $\mathbf{a}$ via solving the Yule-Walker equations [23].

For the Jakes fading, $\mathbf{a}$ is analytically available [1]. In practice, $\mathbf{a}$ is estimated using the fading samples using one of the well-known methods such as Levinson method, Burg method, or Prony method. In a non-stationary environment, the coefficients are frequently updated to follow the model variations.

Here, the linear coefficients are estimated using a Least-Squares approach and solving the equations by the Levinson-Durbin recursion over a window length of $T_{\rm AR}$. The estimates are updated every $T_{\rm AR}$ samples. Fig. 2 shows the flowchart of the algorithm.

B. D-step Versus 1-step Prediction

To perform a D-step prediction, the 1-step predictor could be used D times recursively. However, we are interested in a direct D-step prediction method because it is easier to analyze and to implement. Furthermore, this is particularly helpful in the tracking mode as it is addressed in Section II-C. Equation (11) can be extended to provide a D-step linear predictor [1] as follows

$$\hat{h}_{n+D|n} \;=\; \sum_{i=1}^{N_{\rm AR}} a^{(D)}(i)\,\overline{h}_{n-i+1}. \tag{12}$$

The superscript "(D)" indicates that the variable is related to the D-step predictor (Please note the difference between $a^{(D)}$ which is the D-step predictor coefficient, and a^D which is a to the power of D.). Calculation of the coefficients of the 1-step predictor, $\mathbf{a}$, was explained before. For the D-step predictor,

$$\mathbf{a}^{(D)} = [a^{(D)}(1),\; a^{(D)}(2),\; \cdots,\; a^{(D)}(N_{\rm AR})]^T \tag{13}$$

can be computed using $\mathbf{a}$. From the state-space model, it is shown [24] that $\hat{\mathbf{h}}_{n+D|n} = \mathbf{B}^D\,\mathbf{h}_n$, similar to (9). Hence,

$$\hat{h}_{n+D|n} \;=\; \mathfrak{m}\,\hat{\mathbf{h}}_{n+D|n} \tag{14}$$

$$\;=\; \mathfrak{m}\,\mathbf{B}^D\,\mathbf{h}_n. \tag{15}$$

By comparing (15) and (12) it is observed that

$$\mathbf{a}^{(D)} = (\mathfrak{m}\,\mathbf{B}^D)^T, \tag{16}$$

meaning $\mathbf{a}^{(D)^T}$ is the first row of $\mathbf{B}^D$. Therefore, to obtain the coefficients of the D-step predictor, the calculation steps are as follows: $\mathbf{a} \rightarrow \mathbf{B} \rightarrow \mathbf{B}^D \rightarrow \mathbf{a}^{(D)}$

C. Tracking

In a non-stationary environment, model is changing and the assumption of a fixed model over the observation window results in a performance degradation. A low-complexity adaptive algorithm is desired to track the fine changes of $\mathbf{a}_n$ over time. An LMS algorithm is used as in [4]

$$\mathbf{a}_{n+1} = \mathbf{a}_n + \mu_{\rm AR}\,\mathbf{h}_n^H\,e_n \tag{17}$$

where $e_n = h_n - \hat{h}_n$. Note that we have added the time index n for $\mathbf{a}_n$ in the tracking mode signifying that it is changing at each time step.

As explained in Section II-B, $\mathbf{a}_n^{(D)}$ is calculated using $\mathbf{a}_n$, which requires the calculation of $\mathbf{B}_n^D$. In the tracking mode, this calculation is needed whenever $\mathbf{a}_n$ is updated, which can impose a high computational complexity. In Appendix A, we propose a method to decrease the complexity. Using this method, the final equation for tracking a D-step linear predictor is similar to the LMS algorithm of (17), and is as follows

$$\mathbf{a}_{n+1}^{(D)} = \mathbf{a}_n^{(D)} + \mu_{\mathrm{AR}}\, \mathbf{G}_n^{(D)}\, \mathbf{h}_n^H\, e_n, \tag{18}$$

where $\mathbf{G}_n^{(D)}$ is an $N_{\mathrm{AR}} \times N_{\mathrm{AR}}$ matrix. Appendix A explains the structure and the calculation of $\mathbf{G}_n^{(D)}$.

III. The Proposed Approach

Consider the fading model shown in (2). Assuming a sampling rate of $f_s = 1/T_s$, the fading samples can be written as

$$h_n = \sum_{k=1}^{N_{\mathrm{sc}}} \alpha(k)\, e^{j\omega(k) n T_s} + \zeta_n \tag{19}$$

where $h_n = h(nT_s)$, and n is the time index. In many mobile environments, there are a few main scatterers which construct the fading signal [13]. Whereas in some urban areas there could be up to eight or even more contributing components in the fading signal [25]. In any case, the sum-sinusoidal model of (19) can represent the fading signal. Note that the Jakes model is a special case of the sum-sinusoidal model, and is mathematically valid only for a rich-scattering environment.

A. Estimation of the Model Parameters

Estimation of the parameters of a sum-sinusoidal model is a well-known problem [26], particularly in the areas like acoustic and speech processing, and signal processing in communications. In this work, we are interested in a practical and efficient solution with complexity constraints, for modeling the mobile fading channel.

A majority of the works on channel modeling use a statistical approach to capture the channel behavior. However, the fading model (19) could be observed as a deterministic equation, and a handful of articles

have used this approach to capture the behavior of the fading process, e.g., refer to [18], [19], [20], [21]. Assuming N_{sc} scatterers, there are $2\,N_{\text{sc}}$ unknown parameters to be determined in the model given in (19). As a systematic solution, only $2\,N_{\text{sc}}$ fading samples are required to form an equation set. Solving the equation set provides $\omega(k)$ and $\alpha(k)$, for $k = 1, \cdots, N_{\text{sc}}$. As this approach uses only a few noisy measurements of the fading process, it could result in poor estimation of the parameters. Article [19] uses an ESPIRIT algorithm to find the doppler frequencies, and then solves a set of linear equations using the Least-Squares method to estimate the complex amplitudes. Alternatively, article [18] uses the Root-MUSIC method to find the doppler frequencies. To estimate the amplitudes, the Least Squares and the Bayesian methods are used in [20] assuming that the doppler frequencies are known. As another solution, [20] assumes an AR model for each $\alpha(k)$, estimates the AR coefficients using a Modified Covariance method, and constructs a Kalman filter on the AR model to estimate the amplitudes [20].

In this paper, we propose a new approach to estimate and track the parameters. We utilize the fact that the doppler frequencies usually change slower compared to the complex amplitude variations when the setting of the scattering environment is the same. Generally speaking, this is because the doppler frequency variations are the result of any acceleration of the mobile movement, however the complex amplitudes change even when the mobile is moving at a constant velocity as the distances are changing. A similar observation was made in our simulated fading samples. Therefore, we separate the tracking of $\omega(k)$'s and $\alpha(k)$'s, to capture their different dynamics properly. The details of the proposed method follows.

Assuming a constant scattering model, Fourier transform of the fading signal shown in (19) can provide the estimates of the model parameters, as different scattering components are decoupled in the frequency domain. Fourier analysis can provide an accurate estimation of $\omega(k)$'s if they do not change significantly and the observation window is not too short. In practice, the $\omega(k)$'s change slowly with time. Therefore, a high-resolution method is required to estimate the doppler frequencies using a short window of recent measurements, as in [18], [19], [20]. Furthermore, these estimates need to be performed frequently which imposes a high computational complexity. However, this problem can be solved by an adaptive filter. We

utilize a tracking loop to follow the slow variations of $\omega(k)$'s at each fading sample. Therefore, unlike the window-based methods, the doppler frequencies are up-to-date at each sample. A sudden change in the frequencies may occasionally happen, for example, if the mobile path abruptly changes. In this case, the frequencies are estimated again. Because of the robustness of this approach, the initial estimates of the frequencies do not need to be very accurate. Therefore, we can use a simple Fourier analysis to do this.

Fourier analysis can provide rough estimates for the amplitudes as well. However, $\alpha(k)$'s usually change fast, and these changes may even be significant over a few fading samples. Therefore, a vigilant algorithm is needed for tracking the $\alpha(k)$'s. Knowing $\omega(k)$'s, we construct a Kalman filter based on the sum-sinusoidal model to efficiently follow the $\alpha(k)$ variations. The state-space model is introduced in the next two sections.

B. The State-Space Model

A time evolution model is a useful tool for the prediction of a process. A well-known form of an evolution model known as the state-space model can be written as

$$\begin{cases} \mathbf{x}_n = \mathbf{A}_n \, \mathbf{x}_{n-1} + \mathbf{q}_n \\ \\ z_n = \mathbf{m}_n \, \mathbf{x}_n + v_n \end{cases} \tag{20}$$

where $\mathbf{x}_n$ is an $N_{\text{ray}} \times 1$ state vector at time n which is the sinusoidal channel amplitude vector, $\mathbf{A}_n$ is an $N_{\text{ray}} \times N_{\text{ray}}$ matrix which controls the transition of the state vector in time (sometimes called transition matrix), and $\mathbf{q}_n$ is a noise vector with the covariance $\mathcal{Q}_n = E[\mathbf{q}_n \, \mathbf{q}_n^H]$, which represents the model error. The $\mathbf{m}_n$ is the measurement matrix, v_n is the observation noise, and z_n is the system output (which is substituted by the observed values for implementation). In practical systems, $\mathbf{A}_n$, $\mathcal{Q}_n$ and $\mathbf{m}_n$ are usually constant or slowly time-varying. A well-known state-space representation of an AR model can be found in Section II. We propose a new state-space model for the mobile fading in the following.

Considering the sum-sinusoidal process given in (19), we propose the following state-space model:

$$\mathbf{A}_n = diag \left[e^{j\omega_n(1)\,T_s}, \, e^{j\omega_n(2)\,T_s}, \, \cdots, \, e^{j\omega_n(N_{\text{ray}})\,T_s} \right] \tag{21}$$

and

$$\mathbf{m}_n = [1, \, 1, \, \cdots, \, 1]_{1 \times N_{\text{ray}}}, \tag{22}$$

where $N_{\rm ray}$ is the model order which is the number of the assumed scatterers (ideally, $N_{\rm ray} = N_{\rm sc}$). The z_n in (20) is substituted with the available measurement of the fading sample, i.e., $z_n = \overline{h}_n$. Therefore, the state vector $\mathbf{x}_n$ consists of the complex envelops of the scattering components. A Kalman filter can utilize the state-space model to estimate the state $\mathbf{x}_n$ at each time. An extension of this state-space model to MIMO and multi-path channels is presented in Appendix C.

C. The Proposed Algorithm

Here we propose an adaptive algorithm for fading prediction (which is called "KF"). Fig. 3 shows the flowchart of the algorithm, and a description of the main blocks follows.

1) Kalman Filtering: Kalman Filtering is an estimation method which is commonly used in communication systems (for example, see [11], [27], [12]). Assuming a state-space model, Kalman filter efficiently estimates the state vector $\mathbf{x}_n$ using the observation samples. The estimation of the state vector given the observations at the time n, shown as $\mathbf{x}_{n|n}$, is optimal in the MMSE sense. This estimate is used to predict the future samples of the fading signal.

In the following, the Kalman equations [24] are demonstrated, and Table I defines the variables used in the Kalman equations.

Prediction part:

$$\mathbf{x}_{n|n-1} = \mathbf{A}_n \, \mathbf{x}_{n-1|n-1} \tag{23}$$

$$\mathbf{P}_{n|n-1} = \mathbf{A}_n \, \mathbf{P}_{n-1|n-1} \mathbf{A}_n^T + \mathbf{Q} \tag{24}$$

Update part:

$$\mathbf{k}_n = \mathbf{P}_{n|n-1} \, \mathbf{m}_n^H \, \left(\mathbf{m}_n \, \mathbf{P}_{n|n-1} \, \mathbf{m}_n^H + \sigma_v^2 \right)^{-1} \tag{25}$$

$$\mathbf{x}_{n|n} = \mathbf{x}_{n|n-1} + \mathbf{k}_n \, \left(z_n - \mathbf{m}_n \, \mathbf{x}_{n|n-1} \right) \tag{26}$$

$$\mathbf{P}_{n|n} = \mathbf{P}_{n|n-1} - \mathbf{k}_n \, \mathbf{m}_n \, \mathbf{P}_{n|n-1} \tag{27}$$

The presented Kalman filter works properly as long as the assumed model represented by $\mathbf{A}_n$ is valid. In the transient times when the model is changing, the Kalman filter may lose the track of the state. A

threshold is imposed on the magnitude of the error term in (26), $\epsilon_n = z_n - \mathbf{m}_n \, \mathbf{x}_{n|n-1}$, to prevent large invalid changes. Namely, if $|\epsilon_n| > T_\epsilon$ then $\epsilon'_n = T_\epsilon \, \epsilon_n / |\epsilon_n|$ is used instead. A larger threshold causes less distortion of the error signal in the tracking mode, while a smaller threshold means that the Kalman filter will converge more quickly to the new model when the scattering environment is changing. A threshold of $T_\epsilon = 4 \, \sigma_v$, selected by try and error, is used here. To decrease the transient time, the estimates of $\alpha(k)$'s from the Fourier analysis are applied as initial values to the Kalman filter.

Regarding the computational complexity, this is a low complexity Kalman filter to implement. The inversion of equation (25) is a scaler inversion (not a matrix inversion), and most of the other equations only need vector calculations as $\mathbf{m}_n$ is a constant vector.

2) Model Acquisition: The current parameters for the fading model are estimated according to Section III-A. We apply the Fourier method to estimate $\omega(k), k = 1, \cdots, N_{\text{ray}}$ using an FFT algorithm [1].

Acquisition could be done frequently to keep up-to-date with the doppler frequency changes. To decrease the required computations, it may be done only when the scattering model has significantly changed. The proposed algorithm enters the acquisition mode when the error trend exceeds a threshold as explained in Section III-C5. Furthermore, the algorithm does not allow two consecutive acquisitions to happen very closely (less than T_{Acq} apart), because after each acquisition, other blocks of the algorithm need some time to converge to the new model parameters.

3) Tracking the Doppler Frequencies: An adaptive algorithm is used to track the fine changes of the doppler frequencies. Using a gradient-based approximation, the following LMS algorithm is derived in Appendix D,

$$\omega_{n+1}(k) = \omega_n(k) + \mu_{\text{KF}} \, \Im \left[x^H_{n|n}(k) \, e_n \right], \tag{28}$$

where $\Im$ is the imaginary operator, and

$$e_n \;\; = \;\; z_n - h_{n|n} \tag{29}$$

is the Kalman estimation error, where

$$h_{n|n} \;\; = \;\; \mathbf{m}_n \, \mathbf{x}_{n|n}. \tag{30}$$

Note the entanglement of the two tracking mechanisms which avoids any possible disparity between the doppler frequencies and the amplitudes on a sample by sample basis.

4) Progressive Prediction: Given the current state $\mathbf{x}_n$, which carries all the information about the past, the future channel state should be predicted. It has been shown [24] that given a *constant* state transition matrix $\mathbf{A}_n$, the MMSE estimate of the D-step prediction is

$$\hat{\mathbf{x}}_{n+D|n} = \mathbf{A}_n^D \, \mathbf{x}_{n|n}. \tag{31}$$

where $\hat{\mathbf{x}}_{n+D|n}$ is the estimate of the state vector at the time $n+D$, given the observations until the time n. However, the doppler frequencies slowly change, resulting in slight changes from $\mathbf{A}_{n+1}$ to $\mathbf{A}_{n+D}$. It is shown in Appendix E that considering the model changes over time, the optimal predictor is

$$\hat{\mathbf{x}}_{n+D|n} = \mathbf{A}_{n+D} \cdots \mathbf{A}_{n+2}\mathbf{A}_{n+1} \, \mathbf{x}_{n|n}. \tag{32}$$

At the time n, the matrices $\mathbf{A}_{n+2}, \cdots, \mathbf{A}_{n+D}$ are not known. However, they can be estimated by assuming the same trend for the doppler frequency changes over the next D samples. Utilizing the tracking model of (28), the following estimate is obtained (see Appendix F for the proof),

$$\mathbf{A}_{n+D} \cdots \mathbf{A}_{n+2}\mathbf{A}_{n+1} = \mathbf{A}_n^D \; diag[e^{j\frac{D(D+1)}{2}\delta\mathbf{w}_n T_s}], \tag{33}$$

where

$$\delta\mathbf{w}_n = \mathbf{w}_{n+1} - \mathbf{w}_n \tag{34}$$

which can be calculated using (28).

Using the predicted state $\hat{\mathbf{x}}_{n+D|n}$, the fading sample at the time $n+D$ can be obtained as $\hat{h}_{n+D|n} = \mathbf{m}_n \, \hat{\mathbf{x}}_{n+D|n}$.

5) Calculation of the Error Trend: We use an exponential window for calculation of the error trend from the sample errors as follows

$$E_{n+1} = \lambda \, E_n + (1-\lambda) \, |e_n|^2 , \tag{35}$$

where λ is the forgetting factor ($0 \ll \lambda < 1$). We set the λ to a value that the effect of each error sample is decayed to one percent over the observation window, i.e.,

$$\lambda^{N_{\text{win}}} = 0.01. \tag{36}$$

IV. Implementations and Numerical Results

Table II shows the simulation parameters. We use a wide-sense stationary (WSS) version of the Jakes fading [22] (which uses 14 low-frequency sinusoids) to examine the performance of the underlying algorithms. The Jakes fading is only valid for a rich scattering environment. Furthermore, because the Jakes fading is stationary, it can not model the changes in the scattering environment. To test the algorithms in a more realistic setting, we use a Ray-Tracing (RT) simulation environment as explained in [9]. The mobile is randomly moving vertically and horizontally in the scattering area, comprising of three buildings, and experiences different combinations of signal rays. At each point of the mobile path, it undergoes a different doppler frequency and a different signal power for each ray it receives. The generated fading, called "RT fading", can closely resemble the channel in a real mobile environment, and is used to examine the performance of the algorithms as well. Appendix B includes the pseudo-code for the LP and KF algorithms showing the details of the implementation for the algorithms.

A. Simulation Results

To demonstrate how different parts of the proposed KF algorithm works, we show the results for a sample of RT fading at the mobile speed of $V = 25$ kmph in Figs. 4 - 6 as follows. Fig. 4 and Fig. 5 show the doppler frequencies $\omega_n(k)$'s and the magnitudes of the complex amplitudes $\alpha_n(k)$'s, respectively, and Fig. 6 depicts the trajectories of $|e_n|^2$ and E_n. For the RT fading sample used in this case, the fading environment changes around the time samples of 0.2,1.35,1.55 and 2.0×10^4, corresponding to the times of change in the mobile direction. As explained before, when the scattering environment significantly changes, the algorithm detects the change through the error calculations and enters the acquisition mode. Consequently, the frequency unit, and then the Kalman filter converge to the parameters of the new model. This switch between the acquisition and tracking is clearly observable in the plots at the aforementioned times.

The two prediction algorithms (LP and KF) are compared here, with respect to the average MSE versus the prediction depth. The results are reported for various linear orders $N_{\rm AR}$, and various scattering orders $N_{\rm ray}$, respectively ($N_{\rm ray}$ is an approximation of $N_{\rm sc}$ in (19)). Fig. 7 shows the results for the Jakes fading

for the mobile speeds of $V = 25$ and $V = 100$ kmph. It is observed that KF significantly outperforms LP if N_{ray} is large enough (here, for $N_{\text{ray}} \geq 8$), while LP fails at high prediction depths regardless of the linear order N_{AR}.

Fig. 8 shows the results for RT fading for $V = 25$ and $V = 100$ kmph. It is observed that KF always outperform LP. For a linear predictor, the MSE is directly related to the correlation properties of the fading, i.e., a lower correlation results in a higher MSE. The fading correlation is not monotonic, therefore the MSE versus D plot may not be increasing at high mobile speeds as observed in Fig. 8 for $V = 100$ kmph. It is also observed that increasing N_{ray} does not always improve the performance. In conclusion, the simulations show that the proposed prediction algorithm can perform very well in realistic mobile environments, and it significantly outperforms the adaptive linear algorithm.

V. Conclusion

In this article, we have proposed a new method for prediction of fading channels. The doppler frequencies are estimated and updated by an acquisition-tracking method, and the amplitudes are updated by an improved Kalman filter. Because of its self-recovering nature, the algorithm is robust to the uncertainties such as the changes of the scattering environment, and the accuracy of the channel estimates (i.e., observation SNR). Unlike most Kalman-based methods, the proposed algorithm has a reasonable complexity. Most of the existing algorithms have a window-based structure requiring frequent high-complexity computations, while the proposed method has a sample-by-sample structure resulting in a steady flow of low-complexity calculations. In the tracking mode where algorithms are most of the time, KF has a complexity of the order $(D+20)N_{\text{ray}}$, while LP has a complexity of the order $(D+2)N_{\text{AR}}$. The simulation results show the performance advantage of the KF algorithm over the LP method, especially for long-range predictions.

APPENDIX A
MULTI-STEP TRACKING OF THE AR COEFFICIENTS

Assume that δ_n is the increment vector

$$\mathbf{a}_{n+1} = \mathbf{a}_n + \delta_n. \tag{37}$$

From (37) and (7), we may write

$$\mathbf{B}_{n+1} = \mathbf{B}_n + \Delta_n \tag{38}$$

where

$$\Delta_n = \begin{pmatrix} \delta_n^T \\ \\ \mathbf{0}_{(\mathbf{N}_{\mathrm{AR}}-\mathbf{1})\times\mathbf{N}_{\mathrm{AR}}} \end{pmatrix} \tag{39}$$

For the D-step predictor, we write

$$\mathbf{B}_{n+1}^D = \mathbf{B}_n^D + \Delta_n^{(D)}. \tag{40}$$

The structure of $\Delta_n^{(D)}$ may not exactly be as shown in (39), however, we show the first row of $\Delta_n^{(D)}$ as $\delta_n^{(D)}$.

Assuming a sufficiently large sampling frequency, $\mathbf{a}_n$ is slowly changing with the time index n, and δ_n has a small norm. Therefore,

$$\begin{aligned} \mathbf{B}_{n+1}^D &= (\mathbf{B}_n + \Delta_n)^D & (41)\\ &\cong \mathbf{B}_n^D + \sum_{i=1}^{D} \mathbf{B}_n^{i-1}\Delta_n\mathbf{B}_n^{D-i} & (42) \end{aligned}$$

where (42) is approximated by neglecting the terms in which Δ_n has a power larger than one. Hence,

$$\Delta_n^{(D)} \cong \sum_{i=1}^{D} \mathbf{B}_n^{i-1}\Delta_n\mathbf{B}_n^{D-i} \tag{43}$$

From (40) we may write

$$\mathbf{a}_{n+1}^{(D)} = \mathbf{a}_n^{(D)} + \delta_n^{(D)}, \tag{44}$$

which corresponds to the operation of the first rows of the matrices. Now, $\delta_n^{(D)}$ can be calculated using δ_n as follows,

$$\delta_n \rightarrow \Delta_n \rightarrow \Delta_n^{(D)} \rightarrow \delta_n^{(D)}. \tag{45}$$

It is observed from (43) that each element of $\Delta_n^{(D)}$ is a linear combination of the elements of Δ_n (or equivalently δ_n). Therefore, each element of $\delta_n^{(D)}$ is a linear combination of δ_n and so we can write

$$\delta_n^{(D)} = \mathbf{G}_n^{(D)}\, \delta_n \tag{46}$$

where matrix $\mathbf{G}_n^{(D)}$ represents the linear combinations. Matrix $\mathbf{G}_n^{(D)}$ is a function of $\mathbf{B}_n$ or equivalently a function of the elements of $\mathbf{a}_n$. As an example, equations (47)-(49) show $\mathbf{G}_n^{(D)}$ for $D = 1, 2, 3, 4$, when $N_{\mathrm{AR}} = 3$:

$$\mathbf{G}_n^{(1)} = \begin{pmatrix} 1 & 0 & 0 \\ 0 & 1 & 0 \\ 0 & 0 & 1 \end{pmatrix}, \tag{47}$$

$$\mathbf{G}_n^{(2)} = \begin{pmatrix} 2\, a_n(1) & 1 & 0 \\ a_n(2) & a_n(1) & 1 \\ a_n(3) & 0 & a_n(1) \end{pmatrix}, \tag{48}$$

$$\mathbf{G}_n^{(3)} = \begin{pmatrix} 3\, a_n(1)^2 + 2\, a_n(2) & 2\, a_n(1) & 1 \\ 2\, a_n(1)\, a_n(2) + a_n(3) & 2\, a_n(2) + a_n(1)^2 & a_n(1) \\ 2\, a_n(1)\, a_n(3) & a_n(3) & a_n(1)^2 + a_n(2) \end{pmatrix}, \cdots \tag{49}$$

It is observed that the analytical form of $\mathbf{G}_n^{(D)}$ is more complicated for a larger D. For most applications $\mathbf{a}_n$ is slowly changing, hence $\mathbf{G}_n^{(D)}$ may be recalculated only in the acquisition mode. This approximation can be further simplified if $\mathbf{G}_n^{(D)}$ is calculated for a fixed typical channel. For example, for the channel $\mathbf{a} = [1,\, 0,\, \cdots,\, 0]^T$, $\mathbf{G}_n^{(D)}$ has a simple form; when $N_{\mathrm{AR}} = 3$,

$$\mathbf{G}_n^{(D)} \approx \begin{pmatrix} D & D-1 & D-2 \\ 0 & 1 & 1 \\ 0 & 0 & 1 \end{pmatrix}. \tag{50}$$

Our simulations show that the performance does not change significantly with this approximation in a wide range of mobile speed and D.

APPENDIX B

PSEUDO-CODE FOR THE ALGORITHMS

A. LP Algorithm

L1: **Start**

- Set $n = 0$

L2: **Estimate the LP coefficients**

- Estimate $\mathbf{a}_n$ from the Yule-Walker equations
- Calculate $\mathbf{a}_n^{(D)}$ from (16)
- Set $n_{\mathrm{Acq}} = n$

L3: Set $n = n + 1$

L4: **Linear Prediction**

- Calculate $\hat{h}_{n+D|n}$ by (12)

L5: **Acquisition time?**

- If $n - n_{\mathrm{Acq}} = T_{\mathrm{AR}}$, then Goto L2

L6: **Tracking the LP coefficients**

- Calculate $\mathbf{a}_{n+1}$ by (17)
- Calculate $\mathbf{a}_{n+1}^{(D)}$ from (16)

L7: Goto L3

B. KF Algorithm

L1: **Start**

- Set $n = 0$

L2: **Model Acquisition**

- Estimate $\omega_n(k)$'s and $\alpha_n(k)$'s using FFT
- Calculate $\mathbf{A}_n$ by (21)
- Set $n_{\mathrm{Acq}} = n$

L3: Set $n = n + 1$

L4: **Kalman filter**

- Calculate $\mathbf{x}_{n|n}$ from (23)-(27)

L5: **Predict the state vector**

- Calculate (33)
- Calculate $\hat{\mathbf{x}}_{n+D|n}$ by (32)

L6: **Error check**

- Calculate E_{n+1} by (35)
- If $E_{n+1} \geq E_{\mathrm{Thr}}$ and $n - n_{\mathrm{Acq}} \geq T_{\mathrm{Acq}}$, then Goto L2

L7: **Tracking the Doppler frequencies**

- Calculate (30)
- Calculate the sample error by (29)
- Calculate $\omega_{n+1}(k)$'s by (28)

L8: Goto L3

APPENDIX C
EXTENSION OF THE PROPOSED FADING MODEL

We provided a state-space model for a single-path SISO channel in Section III-B. To extend the model to MIMO and/or multipath channels, the same approach can be used. Assume there is a total of N_{ch} different channels, where each one uses N_{ray} sinusoids. Furthermore, assume that each channel has N_{mp} resolvable multipath. The model can be shown as follows,

$$\begin{cases} \mathbf{X}_n = \mathbf{A}_n \, \mathbf{X}_{n-1} + \mathbf{Q}_n \\ \\ \mathbf{Z}_n = \mathbf{M}_n \, \mathbf{X}_n + \mathbf{V}_n \end{cases} \tag{51}$$

Each variable plays the same role as in (20). $\mathbf{X}_n$ is a $N_{\rm ch}N_{\rm ray} \times N_{\rm mp}$ matrix which is constructed by stacking the state vectors of different channels and different multipath components as follows

$$\mathbf{X}_n = \begin{pmatrix} \mathbf{x}_n(1,1) & \mathbf{x}_n(1,2) & \cdots & \mathbf{x}_n(1,N_{\rm mp}) \\ \mathbf{x}_n(2,1) & \mathbf{x}_n(2,2) & \cdots & \mathbf{x}_n(2,N_{\rm mp}) \\ \vdots & \vdots & & \vdots \\ \mathbf{x}_n(N_{\rm ch},1) & \mathbf{x}_n(N_{\rm ch},2) & \cdots & \mathbf{x}_n(N_{\rm ch},N_{\rm mp}) \end{pmatrix} \tag{52}$$

where $\mathbf{x}_n(i,j)$ is the $N_{\rm ray} \times 1$ state vector of the j-th multipath of the i-th channel. $\mathbf{A}_n$ is a square matrix with $N_{\rm ch}N_{\rm ray}$ diagonal elements containing the doppler frequencies, $\mathbf{Z}_n$ and $\mathbf{V}_n$ are $N_{\rm ch} \times N_{\rm mp}$ matrices which contain the observation and the observation noise for each channel at time n, respectively. $\mathbf{M}_n$ is a $N_{\rm ch} \times N_{\rm ch}N_{\rm ray}$ matrix as depicted in the following,

$$\mathbf{M}_n = \begin{pmatrix} \mathbf{1} & & & \\ & \mathbf{1} & & \\ & & \ddots & \\ & & & \mathbf{1} \end{pmatrix} \tag{53}$$

containing $N_{\rm ch}$ "$\mathbf{1}$"-vectors defined as

$$\mathbf{1} = [1,\, 1,\, \cdots,\, 1]_{1 \times N_{\rm ray}} \tag{54}$$

APPENDIX D

TRACKING ALGORITHM FOR THE DOPPLER FREQUENCIES

Considering the definition of $\mathbf{x}_n$ in (20), from (19) it can be written

$$\hat{h}_n \;=\; \sum_{k=1}^{N_{\rm sc}} x_{n-1}(k)\, e^{j\omega_n(k)T_s}, \tag{55}$$

as the phase-shifts of the sinusoidal terms up to the time $n-1$ are absorbed in $x_{n-1}(k)$. Assume the cost function

$$C_n \;=\; E\left[\left|h_n - \hat{h}_n\right|^2\right] \tag{56}$$

$$\;=\; E\left[|e_n|^2\right], \tag{57}$$

where

$$e_n \;=\; h_n - \hat{h}_n. \tag{58}$$

Hence, a gradient-based tracking algorithm can be implemented as

$$w_{n+1}(k) = w_n(k) - \mu_0 \frac{\partial C_n}{\partial w_n(k)}. \tag{59}$$

To derive the LMS algorithm, we can write

$$\begin{aligned}
\frac{\partial C_n}{\partial w_n(k)} &\approx \frac{\partial \left|e_n\right|^2}{\partial w_n(k)} && (60)\\
&= \frac{\partial (e_n^H\, e_n)}{\partial w_n(k)} && (61)\\
&= 2\,\Re\left[(-j\,T_s\,x_{n-1}(k)\,e^{j\omega_n(k)T_s})^H\, e_n\right] && (62)\\
&= 2\,\Re\left[(-j\,T_s\,x_n(k))^H\, e_n\right] && (63)\\
&= 2\,\Re\left[j\,T_s\,x_n^H(k)\, e_n\right] && (64)\\
&= -2\,T_s\,\Im\left[x_n^H(k)\, e_n\right] && (65)
\end{aligned}$$

where $\Re$ and $\Im$ are the real and imaginary operators, respectively. Equation (60) is obtained by replacing the $E[\cdot]$ of the error term in (57) with the instantaneous value. Now, we can write the LMS algorithm as follows

$$w_{n+1}(k) = w_n(k) + \mu\,\Im\left[x_n^H(k)\, e_n\right], \tag{66}$$

where $\mu = 2\,T_s\,\mu_0$ is the step size.

APPENDIX E

MULTI-STEP PREDICTION OF THE STATE VECTOR

Assume the state-space model shown in (20). The state at the time $n+D$ could be written as

$$\begin{aligned}
\mathbf{x}_{n+D} &= \mathbf{A}_{n+D}\,\mathbf{x}_{n+D-1} + \mathbf{q}_{n+D} && (67)\\
&= \mathbf{A}_{n+D}\,(\mathbf{A}_{n+D-1}\,\mathbf{x}_{n+D-2} + \mathbf{q}_{n+D-1}) + \mathbf{q}_{n+D} && (68)\\
&= \mathbf{A}_{n+D}\mathbf{A}_{n+D-1}\mathbf{x}_{n+D-2} + \mathbf{A}_{n+D}\mathbf{q}_{n+D-1} + \mathbf{q}_{n+D}. && (69)
\end{aligned}$$

Continuing this calculation results in

$$\begin{aligned}\mathbf{x}_{n+D} &= \mathbf{A}_{n+D}\mathbf{A}_{n+D-1}\cdots\mathbf{A}_{n+1}\mathbf{x}_n + \\ &\quad \mathbf{A}_{n+D}\mathbf{A}_{n+D-1}\cdots\mathbf{A}_{n+2}\mathbf{q}_{n+1} + \cdots \\ &\quad + \mathbf{A}_{n+D}\mathbf{q}_{n+D-1} + \mathbf{q}_{n+D} \end{aligned} \tag{70}$$

Hence, for prediction of $\mathbf{x}_{n+D}$ given the available observation data up to the time n, from (70), we have

$$\hat{\mathbf{x}}_{n+D|n} = E\left[\mathbf{x}_{n+D}|\underline{z}_n\right] \tag{71}$$

$$= \mathbf{A}_{n+D}\mathbf{A}_{n+D-1}\cdots\mathbf{A}_{n+1}E\left[\mathbf{x}_n|\underline{z}_n\right] + 0 + \cdots + 0 + 0 \tag{72}$$

$$= \mathbf{A}_{n+D}\mathbf{A}_{n+D-1}\cdots\mathbf{A}_{n+1}\,\mathbf{x}_{n|n} \tag{73}$$

using the fact that $E[\mathbf{q}_i|\underline{z}_n] = 0$, $i > n$.

Finally, the fading sample at the time $n + D$ can be predicted as

$$\hat{h}_{n+D|n} = E\left[h_{n+D}|\underline{z}_n\right] \tag{74}$$

$$= E\left[\mathbf{m}_{n+D}\,\mathbf{x}_{n+D} + v_{n+D}|\underline{z}_n\right] \tag{75}$$

$$= \mathbf{m}_{n+D}\,\hat{\mathbf{x}}_{n+D|n} \tag{76}$$

$$= \mathbf{m}_{n+D}\,\mathbf{A}_{n+D}\mathbf{A}_{n+D-1}\cdots\mathbf{A}_{n+1}\,\mathbf{x}_{n|n}. \tag{77}$$

APPENDIX F
TRACKING THE MULTI-STEP TRANSITION MATRIX

Consider the proposed state-space model described in Section III-B. Implementing (77), it can be written

$$\mathbf{A}_{n+D}\cdots\mathbf{A}_{n+1} = diag\left[e^{j\{\omega_{n+D}(1)+\cdots+\omega_{n+1}(1)\}T_s},\ \cdots,\ e^{j\{\omega_{n+D}(N_{\text{ray}})+\cdots+\omega_{n+1}(N_{\text{ray}})\}T_s}\right] \tag{78}$$

The doppler frequencies are slowly changing. To track these changes, we assume a first order model and use linear extrapolation to write

$$\mathbf{w}_{n+d} \cong \mathbf{w}_n + d\,\delta\mathbf{w}_n, \quad d = 1, 2, \cdots, D. \tag{79}$$

where $\delta\mathbf{w}_n = \mathbf{w}_{n+1} - \mathbf{w}_n$. Consequently,

$$\mathbf{A}_{n+D} \cdots \mathbf{A}_{n+1} = diag\left[e^{j\{D\,\omega_n(1)+(D+\cdots+2+1)\,\delta\omega_n(1)\}T_s}, \cdots, e^{j\{D\,\omega_n(N_{\text{ray}})+(D+\cdots+2+1)\,\delta\omega_n(N_{\text{ray}})\}T_s}\right] \quad (80)$$

$$= \mathbf{A}_n^D \; diag\left[e^{j\frac{D(D+1)}{2}\,\delta\mathbf{w}_n T_s}\right]. \quad (81)$$

REFERENCES

[1] A. Heidari, D. McAvoy, and A. K. Khandani, "Adaptive Long-Range Prediction of Mobile Fading," *The 23rd Biennial Symposium on Communication, Queens University, Kingston, Ontario, Canada*, pp. 219–222, May 2006.

[2] A. Heidari, D. McAvoy, and A. K. Khandani, "Adaptive Channel Prediction System and Method." Filed Canadian and US Patent Application.

[3] G. E. Oien, H. Holm, K. J. Hole, "Impact Of Channel Prediction On Adaptive Coded Modulation Performance In Rayleigh Fading," *IEEE Transactions on Vehicular Technology*, pp. 758 – 769, May 2004.

[4] A. Duel-Hallen and S. Hu, H. Hallen, "Long Range Prediction of Fading Signals: Enabling Adaptive Transmission for Mobile Radio Channels," *IEEE Signal Processing Magazine*, pp. 62–75, May 2000.

[5] A. Heidari, and A. K. Khandani, "Improved Closed-Loop Communication in the Presence of Feedback Delay and Error," *Conference on Information Sciences and Systems (CISS)*, pp. 289–294, Mar. 2006.

[6] A. Heidari and A. K. Khandani, "Closed-Loop Transmit Diversity with Imperfect Feedback," *submitted to IEEE Transactions on Wireless Communications (revised)*, 2007. Available at `http://cst.uwaterloo.ca/~reza`.

[7] T. Svantesson and A.L. Swindlehurst, "A Performance Bound for Prediction of MIMO Channels," *IEEE Signal Processing Magazine*, pp. 520–529, Feb. 2006.

[8] L. Chen and B. Chen, "A Robust Adaptive DFE Receiver for DS-CDMA Systems under Multipath Fading Channels," *IEEE Trans. on Signal Processing*, pp. 1523–1532, July 2001.

[9] A. Heidari, A. K. Khandani, and D. McAvoy, "Channel Prediction for 3G Communication Systems," tech. rep., Bell Mobility, Aug. 2004. Available at `http://cst.uwaterloo.ca/~reza`.

[10] R.J. Lyman, "Optimal Mean-Square Prediction of the Mobile-Radio Fading Envelope," *IEEE Transactions on Signal Processing*, pp. 819–824, Mar. 2003.

[11] C. Komninakis, C. Fragouli, A.H. Sayed, and R.D. Wesel, "Multi-Input Multi-Output Fading Channel Tracking and Equalization Using Kalman Estimation," *IEEE Transactions on Signal Processing*, pp. 1065–1076, May 2002.

[12] M. Yan and B. D. Rao, "Performance of an Array Receiver with a Kalman Channel Predictor for Fast Rayleigh Flat Fading Environments," *IEEE Journal on selected Areas in Communications*, pp. 1164–1172, June 2001.

[13] T. Eyceoz, A. Duel-Hallen, and H. Hallen, "Deterministic Channel Modeling and Long Range Prediction of Fast Fading Mobile Radio Channels," *IEEE Communications Letters*, pp. 254–256, Sept. 1998.

[14] T. Ekman, G. Kubin, M. Sternad, A. Ahlen, "Quadratic And Linear Filters For Radio Channel Prediction," *IEEE 50th Vehicular Technology Conference (VTC'Fall)*, pp. 146 – 150, Sept. 1999.

[15] B. Chen, C. Tsai, and C. Hsu, "Robust Adaptive MMSE/DFE Multiuser Detection in Multipath Fading Channel with Impulse Noise," *IEEE Trans. on Signal Processing*, pp. 306–317, Jan. 2005.

[16] T. S. Rappaport, *Wireless Communications: Principles and Practice*. Prentice-Hall, 1996.

[17] W. C. Jakes, Ed., *Microwave Mobile Communications*. New York: IEEE Press, 1974.

[18] J.K. Hwang and J.H Winters, "Sinusoidal Modeling and Prediction of Fast Fading Processes," *IEEE Global Telecommunications Conference (GLOBECOM'98)*, pp. 892–897, Nov. 1998.

[19] J.B. Andersen, J. Jensen, S.H. Jensen, and F. Frederiksen, "Prediction of Future Fading Based on Past Measurements," *IEEE 50th Vehicular Technology Conference (VTC'Fall)*, pp. 151–155, Sept. 1999.

[20] Y. Liu and D. Pang, "Using the Kalman Filter for Long Range Channel Prediction," Master's thesis, Department of Signals and Systems, Chalmers University of Technology, Goteborg, Sweden, Feb. 2005.

[21] M. Chen, M. Viberg, and T. Ekman, "Two New Approaches to Channel Prediction Based on Sinusoidal Modelling," *13th IEEE/SP Workshop on Statistical Signal Processing*, pp. 697–700, July 2005.

[22] M. F. Pop and C. Beauliu, "Limitations of Sum-of-Sinusoids Fading Channel Simulators," *IEEE Trans. on Communications*, pp. 699–708, Apr. 2001.

[23] A. Papulis, *Probability, Random Variables, and Stochastic Processes*. McGraw-Hill, 1984.

[24] G. Janacek and L. Swift, *Time Series: Forecasting, Simulation, Applications*. Prentice Hall, 1993.

[25] P. A. Matthews and B. Mohebbi, "Direction of Arrival Measurements at UHF," *Electronics Letters*, pp. 1069 – 1070, Aug. 1989.

[26] B. G. Quinn and E. J. Hannan, *The Estimation and Tracking of Frequency*. Cambridge University Press, 2001.

[27] H. Gerlach et al., "Joint Kalman Channel Estimation and Equalization for the UMTS FDD Downlink," *IEEE 58th Vehicular Technology Conference (VTC'Fall)*, pp. 1263–1267, Oct. 2003.

LIST OF FIGURES

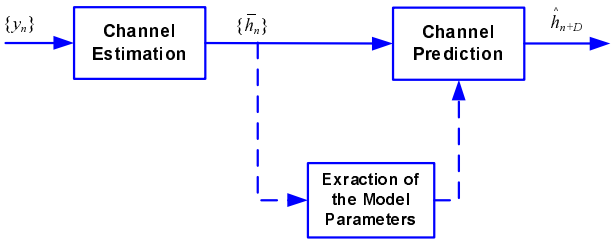

Fig. 1. Block diagram of a channel prediction scheme

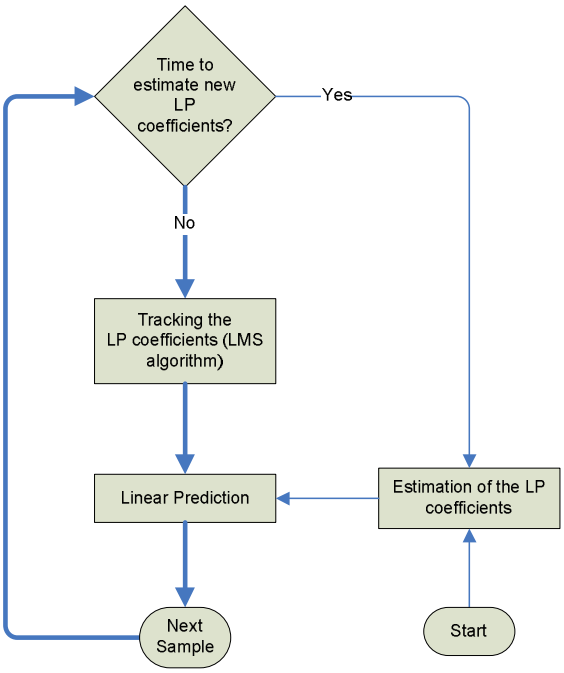

Fig. 2. Block diagram of the linear prediction algorithm (LP)

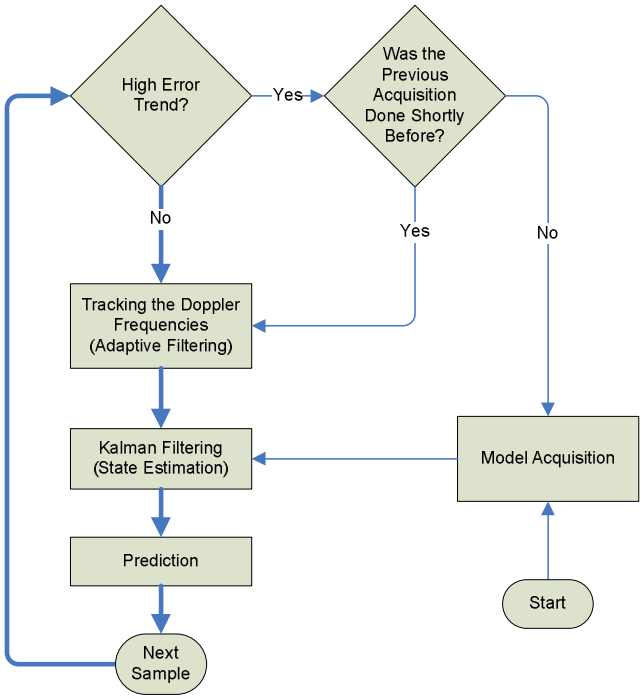

Fig. 3. Block diagram of proposed prediction algorithm (KF)

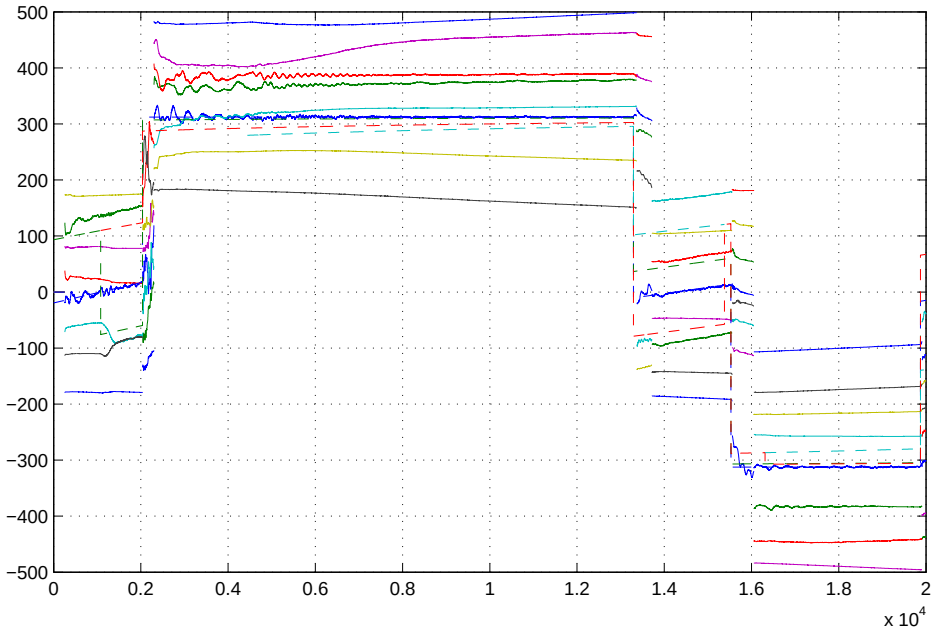

Fig. 4. Estimation and tracking of the doppler frequencies

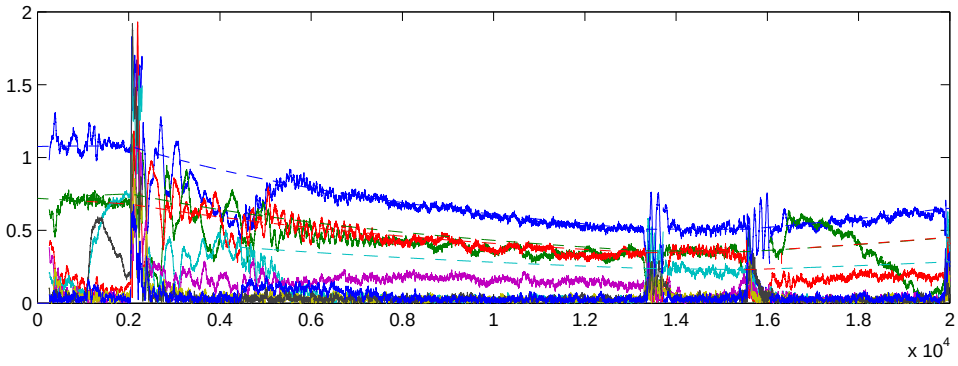

Fig. 5. Kalman tracking of the amplitudes

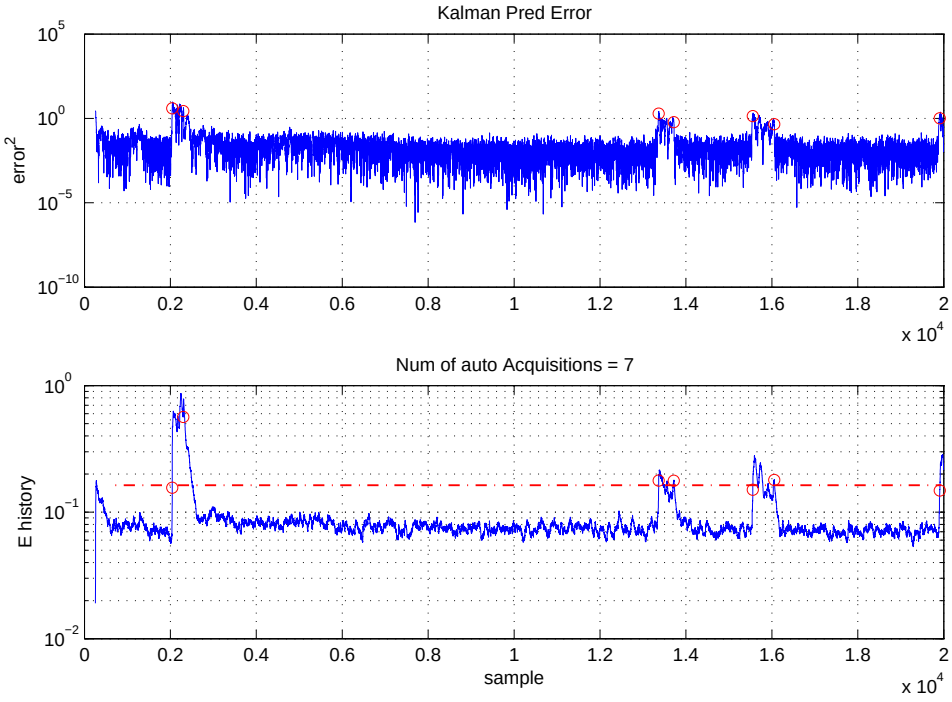

Fig. 6. Error history for the Kalman filter

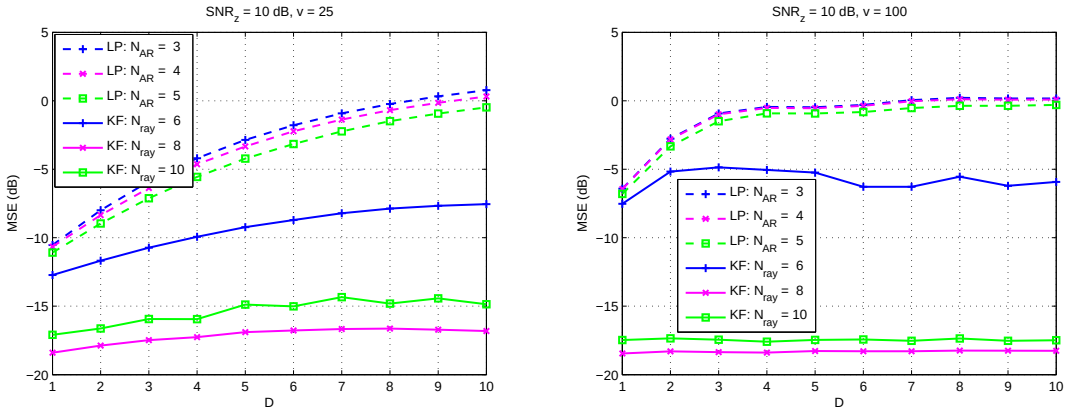

Fig. 7. Comparison of MSE versus prediction depth for the (stationary) Jakes fading at $V = 25$ and $V = 100$

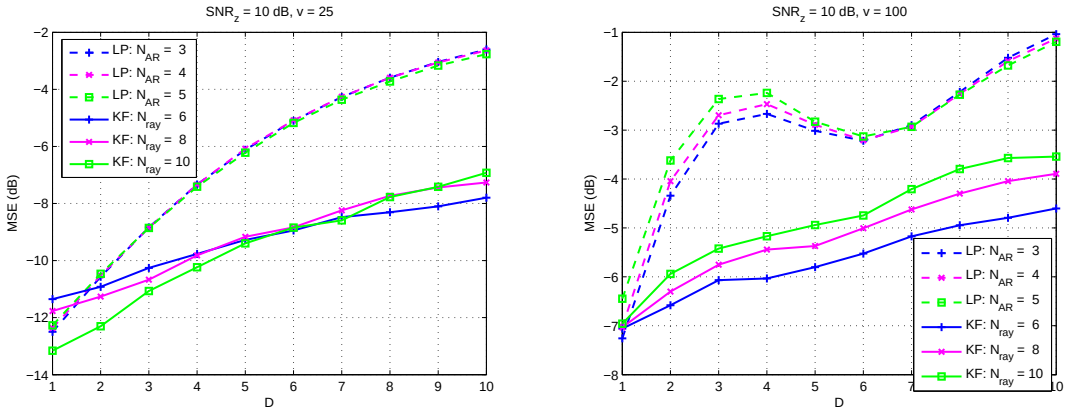

Fig. 8. Comparison of MSE versus prediction depth for (non-stationary) RT fading at $V = 25$ and $V = 100$

LIST OF TABLES

$\mathbf{Q}$	The covariance matrix of the model noise
z_n	The observation sample
$\mathbf{x}_{n\|n-1}$	The *a priori* estimate of the state $\mathbf{x}_n$ (i.e., the estimation of the state at the time n given the observations upto the time $n-1$)
$\mathbf{x}_{n\|n}$	The *a posteriori* estimate of the state $\mathbf{x}_n$ (i.e., the estimation of the state at the time n given the observations upto the time n)
$\mathbf{P}_{n\|n-1}$	The covariance matrix of the *a priori* error
$\mathbf{P}_{n\|n}$	The covariance matrix of the *a posteriori* error

TABLE I
VARIABLES USED IN THE KALMAN FILTER

f_c	2.15 GHz
f_s	1500 Hz
SNR_z	10 dB

TABLE II
SIMULATION PARAMETERS